Mapping the electronic structures of a metalloporphyrin molecule on Au(111) by scanning tunneling microscopy and spectroscopy

Howon Kim,[1] Won-joon Son,[2] Won Jun Jang,[1] Jong Keon Yoon,[1] Seungwu Han,[2] and Se-Jong Kahng[1,*]
[1]*Department of Physics, Korea University, 1-5 Anam-dong, Seongbuk-gu, 136-713 Seoul, Korea*
[2]*Department of Materials Science and Engineering, Seoul National University, Seoul 151-744, Korea*
(Received 9 July 2009; revised manuscript received 9 September 2009; published 3 December 2009)

The intramolecular structure of a Co-porphyrin molecule adsorbed on Au(111) is studied using scanning tunneling microscopy and spectroscopy. As the energy is swept from −2 to +2 eV across Fermi level, the shape of the molecular image dramatically evolves from a two-lobed object to a shape with a bright center and, finally, to a four-lobed object. With the help of first-principles calculations, we explain these distinctive features in terms of the integrated molecular orbitals of a saddle conformation and the contribution of a Kondo state. Based on the molecular structure and the orbitals, we explain why the modification in the electronic states of the molecules by the presence of the substrate is relatively modest.

DOI: 10.1103/PhysRevB.80.245402 PACS number(s): 73.22.−f, 68.37.Ef, 31.15.E−, 68.43.−h

I. INTRODUCTION

Certain naturally abundant molecules may be useful as components in future electronic devices.[1] In particular, porphyrins are ubiquitous in biological systems, being the building blocks for such functional macromolecules as chlorophyll, hemoglobin, and myoglobin, where the core reactions of photosynthesis and the respiratory cycle take place.[2] Because of these molecules' highly conjugated structures and their flexible functional groups, a number of groups are trying to use them in nanoscience and molecular electronics.[3–17] In line with this, the electronic transport properties of porphyrin molecular junctions have been studied extensively and researchers have suggested mechanisms for their negative differential resistance,[4] spin-dependent conductance,[5] and aromaticity control.[6] There are also studies regarding molecule-molecule and molecule-metal interactions that might be important in the fabrication of molecular devices using porphyrins.[11–13] However, understanding the electronic behavior of porphyrins will demand further information on the intramolecular structure and the electronic states of these molecules and the literature in this area is still quite limited.[14]

In this paper, we describe our scanning tunneling microscopy (STM) and scanning tunneling spectroscopy (STS) study of 5-, 10-, 15-, and 20-tetrakis-(4-bromophenyl)-porphyrin-Co (TBrPP-Co) molecules adsorbed on Au(111). The same molecule has recently been studied on Cu(111) with regard to the manipulation of Kondo effect[10,17] while in this study, we focus on the energy-resolved STM images and electronic states in view of molecular orbitals. In our STM images, the molecule exhibits continuous but dramatic shape evolution, which is explained with the help of our first-principles study.

II. EXPERIMENT

Our experiments were performed with a home-built STM system that has a base pressure below 7×10^{-11} torr. Both the STM and the STS measurements were carried out at 80 or 8 K. The Au(111) surface was prepared from a thin film (2000 Å thick) of Au on mica that was exposed to several cycles of Ar-ion sputtering and annealing at 800 K over the course of 1 h. The surface cleanliness of the Au(111) was checked by observing typical herringbone structures on the wide terraces (about 50 nm) in STM images. Commercially available TBrPP-Co (Porphyrin Systems, Germany) was first outgassed in vacuum for several hours and evaporated from an alumina-coated crucible heated at ~500 K. The coverage was monitored with a quartz-crystal monitor and controlled at submonolayer level as confirmed by STM images. The sample deposited with molecules was loaded to the STM head and cooled down to 80 K. STM images were obtained at constant-current mode with a Pt/Rh tip. STS spectra were obtained by a lock-in technique with a modulation voltage of 10 mV_{rms} and at a frequency of 1.5 kHz. The feedback loop was open for STS measurement and closed for the mapping of differential conductance.

III. RESULTS AND DISCUSSION

Figure 1(a) shows an atomic model of the 5-, 10-, 15-, and 20-tetrakis-(4-bromophenyl)-porphyrin-Co molecule. A Co atom (in reality, Co is in the +2 oxidation state) is at the center, linked to a macrocycle consisting of four pyrroline subunits. Four bromophenyl end groups are attached to the macrocycle through σ bonds. The bromophenyl groups have a rotational degree of freedom about the axis of the σ bonds, which allows the molecule to adapt to its local environment.[18] Porphyrin molecules can be a planar geometry and also be distorted in response to an environment. The simplest possible distortion is a saddle conformation in which two pyrroline subunits in the dotted line in Fig. 1(a) protrudes relative to the remaining two pyrroline subunits, causing a shape asymmetry or twofold symmetry.

When the molecules are deposited on Au(111) surface at about 200 K, they are mobile and form molecular islands. Figure 1(b) shows a typical STM image obtained after depositing porphyrin molecules on Au(111). A molecule is identified as a dumbbell or two-lobed shape with four legs, which correspond to the macrocycle and the bromophenyls, respectively. Sometimes a dumbbell shape with one or two

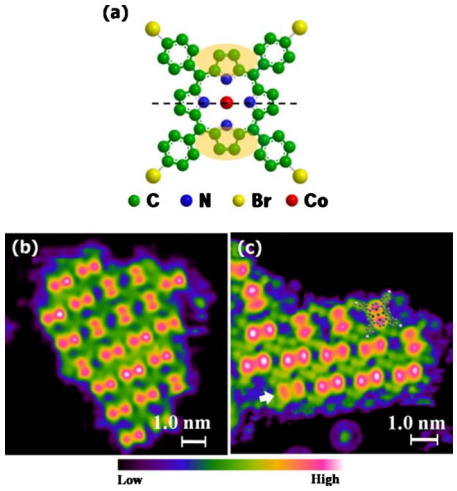

FIG. 1. (Color online) (a) Ball and stick model of an isolated 5-, 10-, 15-, and 20-tetrakis-(4-bromophenyl)-porphyrin-Co(II) molecule. The dotted line represents a distortion axis of this molecule. Two slightly protruding pyrroline subunits are depicted by yellow colored (shaded in black and white) regions. [(b) and (c)] Typical STM images of two-dimensional islands of TBrPP-Co molecules on Au(111) surface. I_T=0.1 nA and V_S=−1.6 V. The white arrow is pointing out the less-rounded molecule, mentioned in the main text. The atomic model from Fig. 1. (a) is superimposed over a single TBrPP-Co(II) molecule in Fig. 1(c). The size of STM images: (b) 9.5 nm×9.5 nm and (c) 8.7 nm×8.7 nm.

less-rounded lobes is observed, such as one at the lower left of the molecular island in Fig. 1(c); this modified shape is possibly the product of local configurations. The molecules show the same trend as others in STM images taken at different energies. The islands are close packed and the molecules on each island line up in one of two preferred orthogonal directions.

It is well known that STM is sensitive to the electronic structure of molecules as well as to their geometric configuration. Figure 2 shows a set of STM images obtained from a molecule at a series of sample biases, or energy levels, between −2 and +2 eV with an incremental energy separation

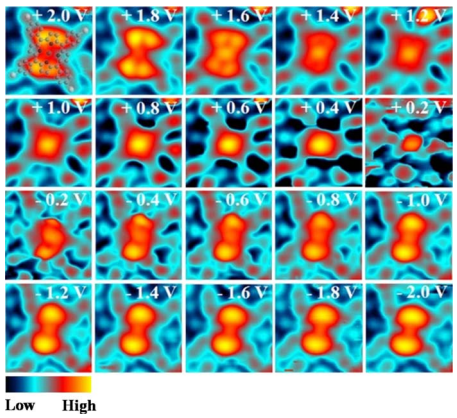

FIG. 2. (Color online) Bias-dependent STM images for an individual TBrPP-Co molecule. I_T=0.1 nA. Sample bias voltages are given at the top of each STM image. The size of all STM images: 1.8 nm×1.8 nm.

of 0.2 eV. While the four legs remain at the same locations in each of the images, the macrocycle of the molecule changes shape substantially. The transformation seems to occur in a reasonably continuous manner as the energy changes, the macrocycle can be seen to take on five distinct shapes as follows: first, at energies between −2.0 and −1.2 eV, the two-lobed shape appears, as can be seen in the island of Fig. 1(b). The lobes at −2.0 eV seem a little bigger and elongated than the lobes at −1.2 eV. Next, at energies between −1.0 and −0.2 eV, a three-lobed shape is visible. As the energy level increases and approaches the Fermi level, the two outer lobes become weak while the center protrusion become prominent, implying that they may have different origins. Third, at energies between +0.2 and +1.4 eV, a bright-center shape appears. At +0.2 eV there is a small bright spot at the center of the molecule; as the energy increases, the spot expands until it becomes a rectangular shape covering the whole macrocycle area. Fourth, at an energy of +1.6 eV, a five-lobed shape can be seen. This can be interpreted as a composition of two different shapes, a four-lobed shape and a bright-center shape. Finally, at energies between +1.8 and +2.0 eV, a four-lobe shape is visible. Among these five shapes, the second and fourth can be thought of as combinations of two of the other shapes. It should be noted that most of the images show twofold rather than fourfold symmetry, even in the four-lobed shape and in the spatial configuration of the four legs, which implies that the molecule is in a saddle rather than a planar conformation. We were unable to find a molecule in planar conformation on Au(111) surface. When molecule adsorb on surfaces, they try to find stable structures that can be accommodated by surface atomic structure. Adsorption configuration and intramolecular structure will be, in general, strongly dependent on the material and orientation of substrate. On Cu(111) and Cu(100), it was reported that TBrPP-Co could form two different kinds of conformations.[10] One of them is a saddlelike structure, showing two lobes at filled state and four lobes at empty-state STM images. Even though available data are not enough to be compared with our experiment, they might have similar energy-dependent behaviors to ours. If then, this molecular conformation would be an example that is not strongly affected by substrate.

In order to understand the observed features, we performed a first-principles calculation based on density-functional theory. The density-functional method has been successfully applied to porphyrin molecules in previous studies.[14,19] We performed spin-polarized density-functional calculations with the VASP code[20] and we used the projector-augmented wave potential[21] and the spin-polarized generalized gradient approximation with the Perdew-Burke-Ernzerhof functional[22] to describe the ion-electron interactions and the exchange correlations between electrons, respectively. The energy cutoff for the plane-wave basis was set to 400 eV. During geometry relaxation, the Hellmann-Feynman force on each atom was reduced to 0.02 eV/Å.

To decide the exact structure of the molecule, we need to take into account the substrate in our calculation and try various kinds of geometrical structures to find the best match to our experimental results. For a first-order approximation, an isolated TBrPP-Co(II) molecule without a substrate was

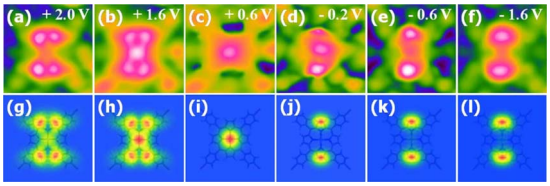

FIG. 3. (Color online) Representative experiment and simulation results of STM images for an individual TBrPP-Co molecule. The experiment results are shown in (a)–(f) and the calculation results for the corresponding sample bias voltages are shown in (g)–(l). A detailed description about the theoretical method used to calculate the images is provided in the text. I_T=0.1 nA.

considered in our simulation study. To obtain the saddle configuration, we began with the geometry obtained in Ref. 6 and then brominated the paraposition of each phenyl ring. Next we displaced the nitrogen atoms linked to the central Co with various degree of distortion and relaxed them without any constraint. Among the locally stable configurations obtained in this way, we chose the most stable one. To simulate the STM image, we employed a relatively large cell of $30\times30\times30$ Å^3. STM images were produced with the Tersoff-Hamann approximation.[23] The images were constructed based on the charge density of the plane lying 4 Å above and parallel to the plane containing the central Co atom. The intensity of each image was renormalized. From this simulation, we want to show how our STM image can be reproduced by our calculations.

Figure 3 shows the simulated results alongside the experimental STM images, which illustrates several distinctive features of the molecule. At the unoccupied energy levels, the simulated results reveal three different structures; a four-lobed shape at +2.0 eV in Fig. 3(a), a five-lobed shape at +1.6 eV in (b), and a bright-center shape at +0.6 eV in (c), which are in excellent agreement with our experimental observations [(g), (h), and (i)]. At the occupied energy levels, on the other hand, the simulated results in Figs. 3(j)–3(l) show mostly two-lobed shapes, which is consistent with the experimental data at −1.6 eV in (f) but not completely consistent at −0.6 and −0.2 eV because the experimental data in (d) and (e) show a three-lobed shape containing a bright center in addition to the two lobes at those energy levels. This difference can be understood when the Kondo effect is taken into account.

Figures 4(a) and 4(b) show STS data obtained at two different locations marked by the dots in the insets. Figure 4(c) shows STS data obtained at bare Au(111) area for comparison which includes strong surface-state onset at around −0.6 eV. In the STS curve obtained at the center of the molecule, a peak is discernible at the Fermi level, as marked by an arrow in Fig. 4(a). This peak is enlarged in Fig. 4(d) and similar to what is seen with the Kondo effect, which occurs when the magnetic spin of an adsorbate is screened by the Fermi electrons of a nonmagnetic substrate, resulting in localized electronic states.[25,26] In our system the Co atom at the center of the molecule possesses a magnetic spin that interacts with the conduction electrons of the Au(111) substrate.[10,17] The Lorenzian-type fitting in Fig. 4(c) is based on the Fano formula, which describes the result of a direct

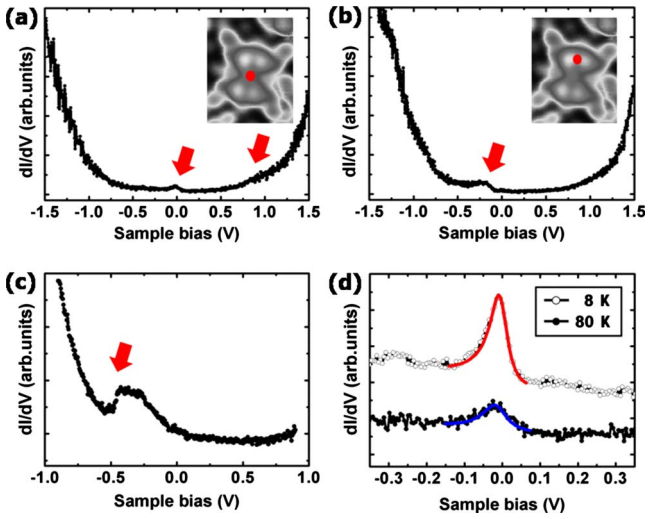

FIG. 4. (Color online) Scanning tunneling spectroscopy results at different locations. Initial tunneling conditions are I_T=0.3 nA and V_s=0.7 V. As represented by the red spots in the STM images, the spectrum in (a) was obtained at the center of the molecule, and the spectrum in (b) at the center of one-protruded pyrroline subunit. The peaks represented by red arrows are explained in the text. The spectrum in (c) was obtained at a bare Au(111) region for comparison showing a well-known surface-state onset at −0.5 eV. (d) The enlarged STS results from (a) under 80 K (filled circle) and 8 K (open circle), respectively. The red and blue solid lines shows a Lorenzian fitting. The fitting parameters for the blue solid line are q=5.0, $E_{K=}$−3.5 meV, and T_K=220 K. (see Ref. 24).

tunneling channel from a tip to a metallic substrate and an indirect channel via magnetic impurity.[24] There are three parameters known as resonance position (ε_K), asymmetry parameter (q), and Kondo effect (T_K). We have confirmed the asymmetric shape of the peak by fitting it in Fig. 4(d) with a Lorentzian-type curve, which results in a Kondo temperature of 230 K. The shape of Kondo resonance state tells us the nature of electron-tunneling process in STM junction. If the tip is more strongly coupled to the Kondo state than to the continuum state of conduction electron, the curve will take a peak shape. On the other hand, if the tip is more strongly coupled to the continuum state, it will have a dip shape. So, on Au(111) where there is a peak, tip prefers Kondo state, while on Cu(111) tip prefers continuum state. It is however complicated question how the preference of tip is determined at present. The Kondo temperatures measured in metallomolecules on metal surfaces span large temperature range. TBrPP on Cu(111) has two different conformation with the Kondo temperature of 130 and 170 K.[10] A bent structure of Co-phthalocyanine on Au(111) has T_K of 200 K (Ref. 27) which is similar to ours. However, there are higher T_K results than these. For example, Fe-phthalocyanine on Au(111) has T_K of 550 K.[28] Based on the experiment on Co-carbonyl species on Cu(100), it was suggested that Kondo temperature increases as the number of ligands to Co atom increases.[29] Recent experiments performed on Pb wedges prepared on Si(111) demonstrated that Kondo temperature can be manipulated by controlling the electron density of states at Fermi level.[30] Since the T_K of TBrPP-Co is higher on

Au(111) than that on Cu(111), the interaction between *d* electron and conduction electron must be stronger on Au(111), or there are more electron density of states at Fermi level on Au(111) than on Cu(111).

Since an STM image is an integrated result of the spatially distributed density of states at the Fermi level to a sample bias, it appears that the weak protrusion at the center of the three-lobe shape was produced by a localized Kondo effect. Therefore, the three-lobed shape in Figs. 3(d) and 3(e) can be regarded as the combination of a center protrusion induced by the Kondo effect and the two lobes of the simulated result that is shown in Figs. 3(j) and 3(k). It should be noted that Kondo effect is technically beyond the limits of a first-principles simulation because screening is inherently a many body phenomenon. In the unoccupied states, the bright center that appears at +0.2 eV in Fig. 2(c) may result from the same mechanism as the Kondo effect, which would mean that the bright-center shape has two different origins, the Kondo effect and a molecular state. The energy location of highest occupied molecular orbital (HOMO) which must be related to Co *d* level is a little higher than that reported in Cu(111) case where it was assigned at −0.7 eV.[10] This may be due to the work-function difference between Au and Cu. Indeed, there is a report where Co *d* level is assigned to −0.1 eV in the case of Co-TPP on Au(111).[11] The energy difference can also be made by delicate structural details. In Cu(111) case, besides the molecular structure with the *d* level at −0.7 eV, there is another molecular structure which does not show any *d*-level-related feature.[10] Also, in Co-TPP on Cu(111), no state related to *d* level was observed, even if the molecular structure is similar to ours.[14] In any case, *d*-level-related HOMO is close to Fermi level on Au(111) so that they can have strong enough interaction, resulting in higher Kondo temperature than on Cu(111).

The fundamental feature underlying an STM image can be thought of as the object's molecular electronic states or orbitals. Those can be measured as maps of differential conductance of tunneling current, which corresponds to local density of states (LDOS). Figure 5 shows several LDOS maps together with the molecular orbitals (top and side views). LDOS maps were measured by the lock-in method keeping the feedback on, and the orbitals were calculated by the density-functional method. In the occupied levels, LDOS maps show two-lobed shapes at −0.2 and −0.6 eV in Figs. 5(c) and 5(d). They correspond to calculated HOMO at −0.24 eV and HOMO-1 at −0.57 eV in molecular states, respectively. In the unoccupied levels, LDOS map show a bright-center shape at +0.6 eV [Fig. 5(b)] and a four-lobed shape at +1.5 eV [Fig. 5(a)]. These correspond to calculated lowest unoccupied molecular orbitals (LUMO) at 0.26 eV and LUMO+1 at 1.32 eV, respectively. If only the top views of the molecular orbitals are considered, they may seem to have almost a fourfold symmetry, making it difficult to imagine where the asymmetry or the twofold symmetry of the LDOS maps comes from. In fact, we observed in our simulation that most spatial and energetic characteristics of the molecular state are the same in the planar and the saddle configuration, except for the bending distortion that occurs in the saddle configuration. By looking at the molecular orbitals in side view, as shown in Figs. 5(i)–5(l), one can more easily

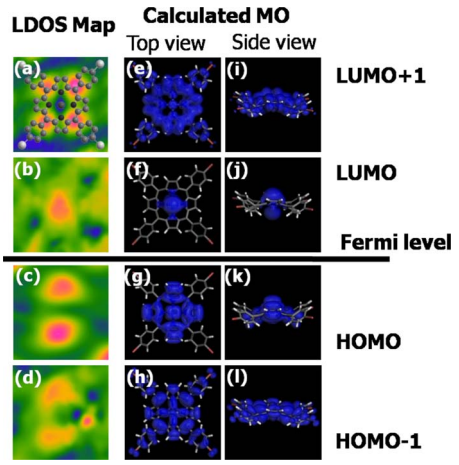

FIG. 5. (Color online) The experiment results of the LDOS maps [the first column: (a)–(d)] and the calculated molecular orbitals for a TBrPP-Co(II) [the second column for top views (e)–(h)] and the third column for side views [(i)–(l)]. I_T=0.1 nA. The applied sample bias voltages are (a) +1.5 V, (b) +0.6 V, (c) −0.2 V, and (d) −0.6 V. The energy levels of calculated molecular orbital are −0.57 eV (HOMO-1), −0.24 eV (HOMO), +0.26 eV (LUMO), and +1.32 eV (LUMO+1).

recognize the shapes of the LDOS map. For example, in Fig. 5(k), out of four pyrroline subunits, only two are protruding, while the other two are receding. One can see that the part of a orbital around the center stands out more as compared with the part around the other two, showing that the two-lobed (HOMO and HOMO-1) and the four-lobed (LUMO+1) structures agree well with the measured LDOS map. It should be noticed that the four lobes did not make fourfold symmetry but twofold which can be explained by the saddle distortion.

In Fig. 5, the LDOS map at +1.5 V shows four-lobed shape which is related to LUMO+1 and originate from the methine bridges and the pyrroline subunits. The methine bridges connect three carbon atoms forming the joints between the macrocycle and bromophenyles. This four-lobed orbital will be responsible not only for the four- and five-lobed shape in the STM image of Fig. 2 but also for the gradual shape change from +0.4 eV (circular) to +1.2 eV (rectangular). Two-lobed shapes in the LDOS map, on the other hand, originate mostly from the two pyrroline subunits and are connected to HOMO and HOMO-1. In Fig. 5, one pyrroline subunit in HOMO consists of two parts while it consists of four parts in HOMO-1. The two and four parts at a pyrroline subunit will be merged as one lobe in LDOS maps due to limited spatial resolution. Since a lobe made of four parts will occupy more space and elongated than that of two parts, the consideration of the orbitals clearly explains the subtle shape evolution happened in two-lobed shapes in Fig. 2; each lobe becomes larger and elongated as energy decreases to −2 eV. In the STS data of Fig. 4, HOMO is observed at −0.2 eV as a peak as marked by an arrow in Fig. 4(b) and LUMO is observed at +0.8 eV in Fig. 4(a). The HOMO-1 and LUMO+1 are believed to be embedded in the steep increase at $|V_S|>1$ eV. In the previous STS experiment on Cu(111), relatively small HOMO-LUMO gap com-

pared with gas phase one was observed similar to ours presumably due to induced dipoles.[14] Still experimentally measured gap, 1.0 eV in STS is larger than the calculated gap, 0.5 eV (HOMO at −0.24 eV and LUMO at 0.26 eV), which is possibly due to the well-known limitation of the density-functional approach.

Up to now, we have discussed what is observed at the aromatic central part of molecule which is consistent with the simulation results. We will briefly discuss the result in the bromophenyl legs. In Fig. 3, the four legs are well identified at every STM image while they are invisible in simulation results. Since the legs are at the location where molecules make contacts with the substrate, there can be some modification from the molecular orbitals at legs such as hybridization and electron donation which is not included in our simulation. In fact, it is amazing that, regardless of what is happening at the legs, the experiment and the simulation results agree so nicely at the macroscycle. It was proposed that a main body of a molecule could be semi-isolated from the substrate by having a landerlike structure,[31,32] where a main body was supported by four or more landing legs just like vehicles. Since the bromophenyles of our TBrPP-Co molecule have the rotational degree of freedom in σ bonds and tend to have extra-bending mechanisms to the surface, the molecule may adsorb like a lander, without having a direct contact between the macrocycle and Au(111) surface. At the same time, as shown in the molecular orbitals in Fig. 5, the lobes at the macrocycle are often disconnected from those at the legs. This is in accordance with the fact that both the macrocycle and the legs maintain their own aromatic rings with 22 and six π electrons, fulfilling Hückel rule, respectively. They are weakly coupled, electronically as well as geometrically, through the σ bonds, providing a reasonable isolation between a macrocycle and a substrate.

Based on photoemission spectroscopy experiments, it was reported that the electronic interaction between the cobalt ion and the surface in TPP-Co/Ag(111) system results in a transfer of electron density from the surface to the ion.[33] The strength of such interaction is strongly dependent on the distance from a substrate to a metal ion. Since Br-C bond is longer than the C-H bond in a bromobenzene molecule by 0.08 nm,[34] the distance from TBrPP-Co to a surface will be larger than that from TPP-Co to a surface. Consequently, an interaction between Co ion and a Au(111) surface is relatively weak in TBrPP/Au(111) and the Co ion is isolated from the substrate.

IV. CONCLUSIONS

The intramolecular structure of metalloporphyin molecules adsorbed on Au(111) has been studied using STM, STS, and first principles simulation. As the energy increases from −2 to +2 eV, the molecular STM images move through a series of five different shapes. Of these, three are associated with independent molecular states. In order to understand the images around the Fermi level, one must take into account the Kondo effect. The bending structure of saddle conformation accounts for the directional asymmetry that is observed in all of the energy levels. Our study shows that the molecular states of porphyrin are not severely altered in the presence of Au(111) but slightly modified by the Kondo effect. As an outlook for future molecular spintronic application, it would be worth to find a way to control the Kondo effect utilizing intramolecular and intermolecular interaction in metalloporphyrin system.

ACKNOWLEDGMENTS

The authors acknowledge financial support from the Korean Government (Grants No. KRF-2004-005-C00060, No. R01-2007-000-11545-0, and No. M10503000187-05M0300-18710) and from a Korea university grant. W.S. and S.H. were supported by a SRC program (Quantum Metamaterials Research Center under Grant No. R11-2008-053-03001-0). We thank W. Ho for providing the design of STM. W.S. thank W. Auwärter and A. Weber-Bargioni for providing the geometries of TPP-Co in Ref. 14.

*Corresponding author; sjkahng@korea.ac.kr

[1] *Functional Organic Materials: Syntheses, Strategies and Applications*, edited by Thomas J. J. Müller and Uwe H. F. Bunz (Wiley-VCH, Weinheim, 2007).
[2] J. P. Collman, R. Boulatov, C. J. Sunderland, and L. Fu, Chem. Rev. **104**, 561 (2004).
[3] H. Tanaka, T. Yajima, T. Matsumoto, Y. Otsuka, and T. Ogawa, Adv. Mater. (Weinheim, Ger.) **18**, 1411 (2006).
[4] M. Q. Long, K.-Q. Chen, L. Wang, W. Qing, B. S. Zou, and Z. Shuai, Appl. Phys. Lett. **92**, 243303 (2008).
[5] Y. Chen, A. Prociuk, T. Perrine, and B. D. Dunietz, Phys. Rev. B **74**, 245320 (2006).
[6] S. U. Lee, R. V. Belosludov, H. Mizuseki, and Y. Kawazoe, Small **4**, 962 (2008).
[7] T. A. Jung, R. R. Schlittler, J. K. Gimzewski, H. Tang, and C. Joachim, Science **271**, 181 (1996).
[8] Q. Li, S. Yamazaki, T. Eguchi, Y. Hasegawa, H. Kim, S.-J. Kahng, J. F. Jia, and Q. K. Xue, Nanotechnology **19**, 465707 (2008).
[9] X. H. Qiu, G. V. Nazin, and W. Ho, Phys. Rev. Lett. **93**, 196806 (2004).
[10] V. Iancu, A. Deshpande, and S.-W. Hla, Nano Lett. **6**, 820 (2006).
[11] L. Scudiero, D. E. Barlow, U. Mazur, and K. W. Hipps, J. Am. Chem. Soc. **123**, 4073 (2001).
[12] J. Otsuki, E. Nagamine, T. Kondo, K. Iwasaki, M. Asakawa, and K. Miyake, J. Am. Chem. Soc. **127**, 10400 (2005).
[13] L. Grill, M. Dyer, L. Lafferentz, M. Persson, M. V. Peters, and S. Hecht, Nat. Nanotechnol. **2**, 687 (2007).
[14] A. Weber-Bargioni, W. Auwärter, F. Klappenberger, J. Reichert, S. Lefrançis, T. Strunskus, C. Wöll, A. Schiffrin, Y. Pennec, and J. V. Barth, ChemPhysChem **9**, 89 (2008).

[15] T. Yokoyama, S. Yokoyama, T. Kamikado, and S. Mashiko, J. Chem. Phys. **115**, 3814 (2001).
[16] W. Auwärter, A. Weber-Bargioni, A. Schiffrin, A. Riemann, O. Gröning, R. Fasel, and J. V. Barth, J. Chem. Phys. **124**, 194708 (2006).
[17] V. Iancu, A. Deshpande, and S.-W. Hla, Phys. Rev. Lett. **97**, 266603 (2006).
[18] J. A. Shelnutt, X.-Z. Song, J.-G. Ma, S.-L. Jia, W. Jentzen, and C. J. Medforth, Chem. Soc. Rev. **27**, 31 (1998).
[19] M.-S. Liao and S. Scheiner, J. Chem. Phys. **117**, 205 (2002).
[20] G. Kresse and J. Hafner, Phys. Rev. B **47**, 558(R) (1993); **49**, 14251 (1994).
[21] P. E. Blöchl, Phys. Rev. B **50**, 17953 (1994).
[22] J. P. Perdew, K. Burke, and M. Ernzerhof, Phys. Rev. Lett. **77**, 3865 (1996).
[23] J. Tersoff and D. R. Hamann, Phys. Rev. B **31**, 805 (1985).
[24] U. Fano, Phys. Rev. **124**, 1866 (1961).
[25] J. Li, W.-D. Schneider, R. Berndt, and B. Delley, Phys. Rev. Lett. **80**, 2893 (1998).
[26] V. Madhavan, W. Chen, T. Jamneala, M. F. Crommie, and N. S. Wingreen, Science **280**, 567 (1998).
[27] A. Zhao, Q. Li, L. Chen, H. Xiang, W. Wang, S. Pan, B. Wang, X. Xiao, J. Yang, J. G. Hou, and Q. Zhu, Science **309**, 1542 (2005).
[28] L. Gao, W. Ji, Y. B. Hu, Z. H. Cheng, Z. T. Deng, Q. Liu, N. Jiang, X. Lin, W. Guo, S. X. Du, W. A. Hofer, X. C. Xie, and H.-J. Gao, Phys. Rev. Lett. **99**, 106402 (2007).
[29] P. Wahl, L. Diekhöner, G. Wittich, L. Vitali, M. A. Schneider, and K. Kern, Phys. Rev. Lett. **95**, 166601 (2005).
[30] Y.-S. Fu, S.-H. Ji, X. Chen, X.-C. Ma, R. Wu, C.-C. Wang, W.-H. Duan, X.-H. Qiu, B. Sun, P. Zhang, J.-F. Jia, and Q.-K. Xue, Phys. Rev. Lett. **99**, 256601 (2007).
[31] F. Rosei, M. Schunack, P. Jiang, A. Gourdon, E. Laegsgaard, I. Stensgaard, C. Joachim, and F. Besenbacher, Science **296**, 328 (2002).
[32] F. Moresco and A. Gourdon, Proc. Natl. Acad. Sci. U.S.A. **102**, 8809 (2005).
[33] T. Lukasczyk, K. Flechtner, L. R. Merte, N. Jux, F. Maier, J. M. Gottfried, and H.-P. Steinrück, J. Phys. Chem. C **111**, 3090 (2007).
[34] A. de la Cruz, J. Campos, and M. Ortiz, J. Mol. Spectrosc. **180**, 305 (1996).